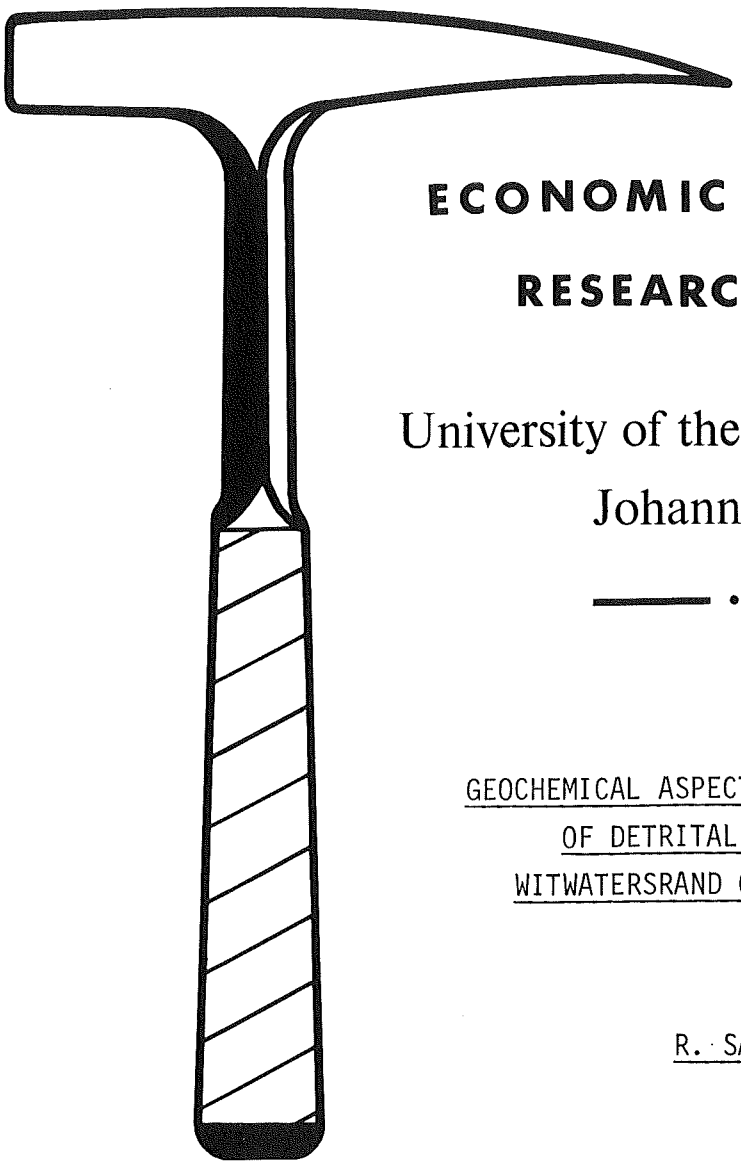

ECONOMIC GEOLOGY RESEARCH UNIT

University of the Witwatersrand
Johannesburg

GEOCHEMICAL ASPECTS OF THE ORIGIN OF DETRITAL PYRITE IN WITWATERSRAND CONGLOMERATES

R. SAAGER

INFORMATION CIRCULAR No. 105

UNIVERSITY OF THE WITWATERSRAND
JOHANNESBURG

GEOCHEMICAL ASPECTS OF THE ORIGIN OF DETRITAL PYRITE IN WITWATERSRAND CONGLOMERATES

by

R. SAAGER

(Visiting Research Fellow from the Institute of Mineralogy and Petrology, University of Heidelberg, West Germany)

ECONOMIC GEOLOGY RESEARCH UNIT

INFORMATION CIRCULAR No. 105

October, 1976

GEOCHEMICAL ASPECTS OF THE ORIGIN OF DETRITAL PYRITE IN WITWATERSRAND CONGLOMERATES

ABSTRACT

The principal source-area of the Witwatersrand sediments, including heavy minerals such as gold, uraninite, and pyrite, lies to the northwest of the basin of deposition. This area is overlain by younger rocks, which makes the location of the actual source virtually impossible. On the basis of a hypothetical provenance model, it has earlier been suggested that the primary source of the sediments was in the Archean granite-greenstone terrane of the Kaapvaal Craton.

In the present study, 57 pyrite samples from primary gold deposits in the greenstone terrane (Swaziland Sequence) and from various gold reefs in the Witwatersrand deposit were investigated with respect to their trace-element content (Co, Ni, Cu, Zn, Pb, Ag) in order to detect the possible presence of similar geochemical trends within both groups of pyrite. The analytical data were treated by statistical methods, and the results indicate that both the primary and the detrital Witwatersrand pyrites, with respect to the investigated elements, were drawn from the same population. They are both clearly different from the Witwatersrand pyrites formed *in situ*. Lead isotopic investigations of sulfides from primary gold deposits in the Swaziland Sequence and of detrital, as well as authigenic, pyrites from the Witwatersrand deposit show a similar isotopic composition of the lead. The results of the present geochemical studies thus constitute strong evidence that the Archean greenstone belts of the Kaapvaal Craton were the most probable source of the detrital pyrites, and also of the gold, in the sediments of the Witwatersrand Basin.

* *

GEOCHEMICAL ASPECTS OF THE ORIGIN OF DETRITAL PYRITE IN WITWATERSRAND CONGLOMERATES

CONTENTS

——————— oOo ———————

ISBN 0 85494 412 5

GEOCHEMICAL ASPECTS OF THE ORIGIN OF DETRITAL PYRITE IN WITWATERSRAND CONGLOMERATES

INTRODUCTION AND GEOLOGICAL SETTING

For many placer deposits, the question of the original source of the heavy minerals is an intriguing, and often hotly-debated, subject of discussion. The solution of the problem is not only of greater academic interest but, in many instances, has proved to be of considerable economic importance.

In the case of the early Precambrian fossil placers of the Witwatersrand Basin in South Africa, the problem of the provenance of the gold, uraninite, and other detrital conglomerate constituents was overshadowed for a long time by the metallogenetic controversy between the hydrothermalists and the placerists (see Becker, 1909; Mellor, 1916; Young, 1917; Graton, 1930; Liebenberg, 1955; Ramdohr, 1955; Davidson, 1957, 1960, and 1961).

A great number of sedimentological, geological, and mineralogical studies carried out during the last twenty years has led to the general acceptance of the *modified placer theory* as a metallogenetic concept for the Witwatersrand deposit. It is believed that, subsequent to their deposition, some of the detrital minerals, notably gold and the sulfides, were reconstituted and lost their water-worn shapes as a result of low-grade regional metamorphism. Most investigators of the Witwatersrand deposits agree that the sediments and heavy minerals originated in a source-area situated to the northwest of the basin of deposition, with only minor amounts of sedimentary material being introduced from the southeastern edge of the Witwatersrand Basin (Pretorius, 1974). Evidence for this conclusion includes the conspicuous occurrence of all the producing goldfields along the northwestern arc of the Witwatersrand Basin, the asymmetry of the gradients of the palaeoslopes, which are considerably steeper on the northwestern side of the basin, and the distinct decrease of conglomerate thickness and pebble size in a southeasterly direction. Pretorius (1966 and 1974) convincingly demonstrated that each of the six major goldfields represents a fluvial fan or fan-delta (Figure 1). Furthermore, he concluded that the fluvial system operated over a short distance,

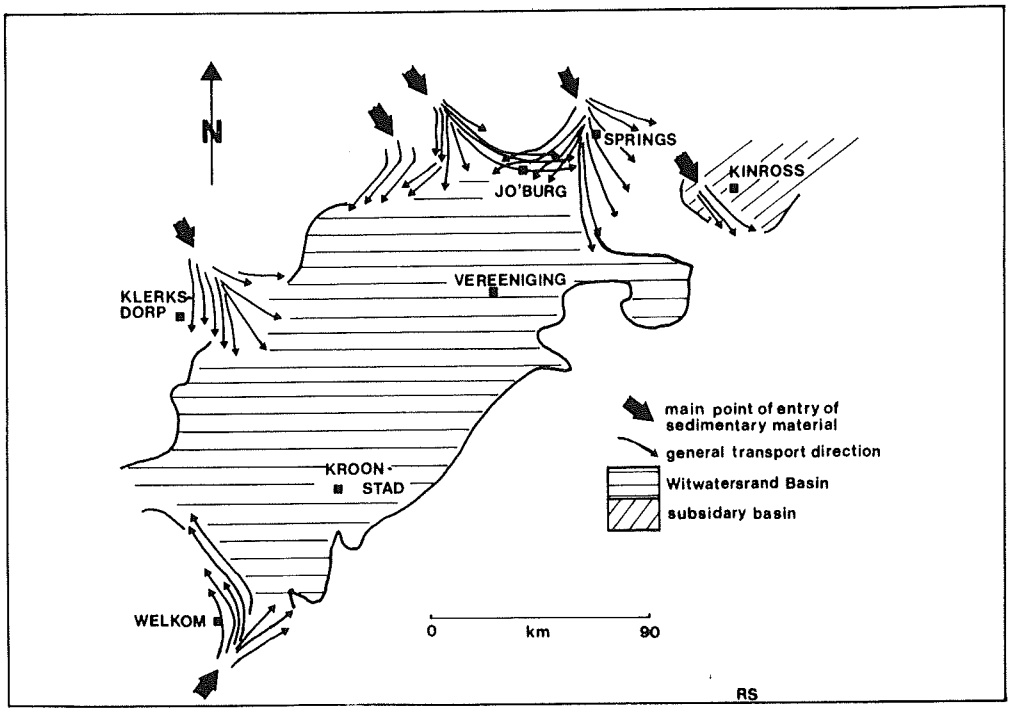

Figure 1 : Situation of main points of entry of sedimentary material into the Witwatersrand Basin and general transport directions (after Brock and Pretorius, 1964).

with the provenance-area close to the edge of the basin of deposition. The entry points of sedimentary material into the basin, corresponding to the apices of the fans, remained relatively fixed during a considerably long period of time, e.g. from Dominion Reef to Upper Witwatersrand times.

To pinpoint the actual provenance-area of the sediments and the placer minerals, however, is virtually impossible, as this area is largely covered by younger Proterozoic rocks, such as the Ventersdorp lavas, the Transvaal sediments, and the Bushveld Igneous Complex. The few windows in which pre-Witwatersrand rocks are exposed, e.g. the Johannesburg Dome, the Westerdam Dome, and the Amalia Dome, show only rock-types similar to those found in the Archean basement of the Eastern Transvaal Lowveld and no other pre-Witwatersrand sequences.

Viljoen et al. (1970), after synthesizing recently published data on the Witwatersrand Basin and on the basement of the Kaapvaal Craton, suggested that the primary source of the Witwatersrand gold and detrital sulfides should be sought in the Archean greenstone belts of the craton. As a hypothetical model of the source-terrane, they proposed the classic area of the Barberton Mountain Land (Figure 2).

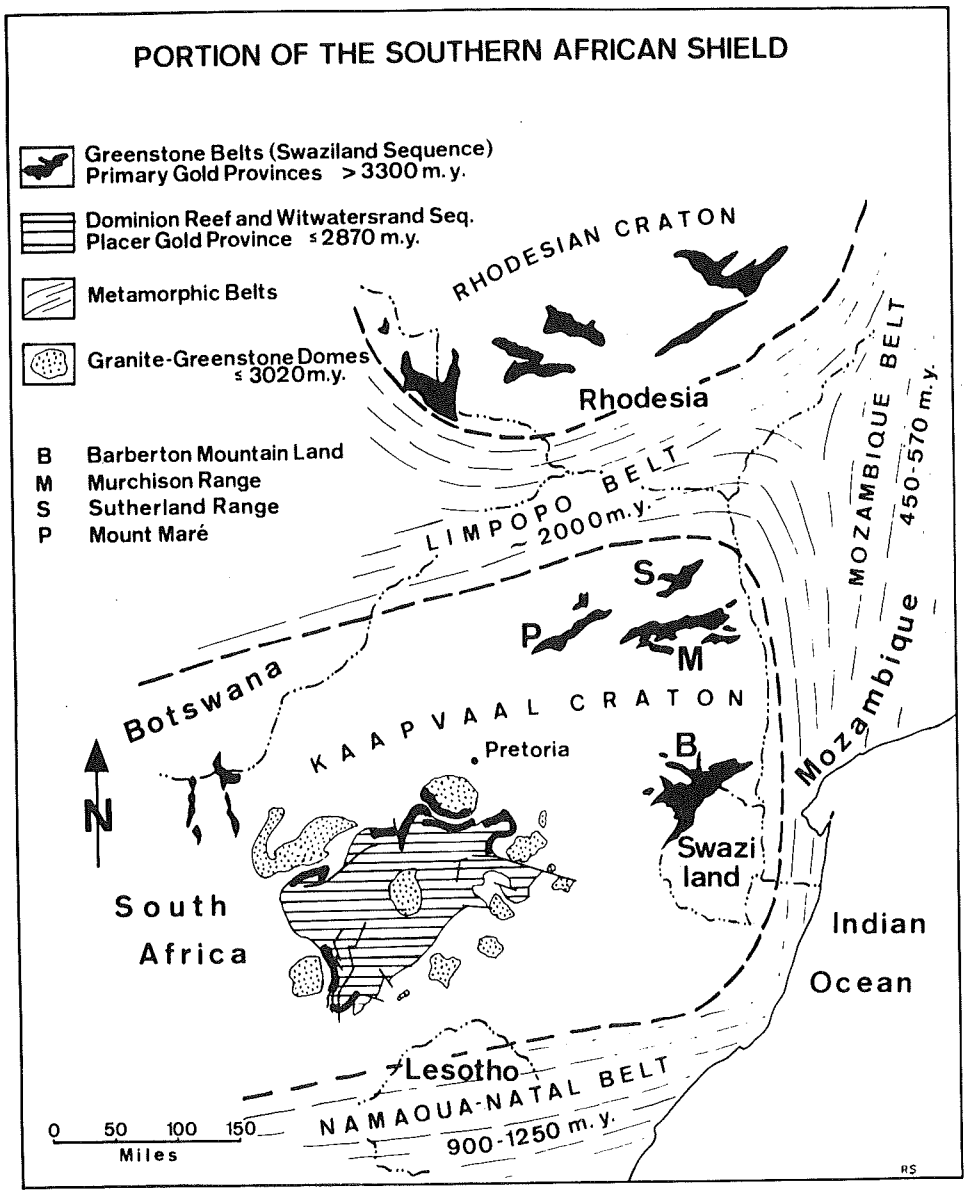

Figure 2 : General geological setting of the Witwatersrand Basin and of the main Archean greenstone belts of the Kaapvaal Craton. The location of the major goldfields along the western and northern rim of the Witwatersrand Basin is marked with a heavy black line.

In the Kaapvaal Craton, the generally northeast-trending Archean greenstone assemblages are referred to as the Swaziland Sequence. The lowermost members of this sequence, which are fully preserved in the Barberton area, constitute the Onverwacht Group. It is characterized by ultramafic, mafic, and acid volcanics (Viljoen and Viljoen, 1969; Anhaeusser, 1971). These rocks are overlain by the argillaceous sediments of the Fig Tree Group which, in turn, is followed by the principally arenaceous sediments of the Moodies Group, forming the topmost members of the sequence. As with other greenstone belts in the Kaapvaal Craton, the Barberton Mountain Land is well mineralized and forms, next to the Witwatersrand Basin, the most important gold province in South Africa (Figure 2).

Most of the gold mineralization in the Barberton Mountain Land is located along a stratigraphic horizon in basic volcanics at the base of the Upper Onverwacht Group and along unconformities between the Upper Onverwacht Group and the sedimentary groups of the Swaziland Sequence. Viljoen et al. (1969) showed that the gold content of the ultramafic and mafic Mg-rich volcanics in the Barberton Mountain Land varies between 0,005 and 0,01 ppm. Gold values of up to 0,112 ppm have been observed where the rocks have been weathered and recycled. The gold content in the accompanying intrusive basement granites, on the other hand, is less than 0,005 ppm. From these geochemical trends and from various geological and mineralogical observations, Viljoen et al. (1969) and Saager (1973a and 1973b) concluded that the gold deposits in the greenstone belts are genetically related to the Mg-rich mafic-to-ultramafic volcanics and not to the late volatile phases of the intruding granites. Descriptions of the various processes which led to the formation of the gold deposits in the greenstone belts of the Kaapvaal Craton are given by Viljoen et al. (1969) and Saager (1973b).

The suitability of the Barberton Mountain Land as a model source-terrane for the sedimentary filling of the Witwatersrand Basin was demonstrated by Viljoen et al. (1970) through the correlation between the expected heavy minerals derived from successive erosional levels of such a terrane and the actual heavy minerals encountered in the various horizons of the Witwatersrand sediments. The results of their study are summarized in Table 1 which demonstrates the relative abundances of uraninite, monazite, cassiterite, and garnet in the lower portions of the sedimentary succession, especially in the conglomerates of the Dominion Reef Sequence. Chromite and the platinoids show a distinct increase towards the topmost members of the sediments, and the gold and the sulfides reach a maximum in the Main-Bird Group of the Upper Witwatersrand Division. This heavy mineral distribution indicates that, in the provenance-area, the lower erosional level consisted mainly of mafic-to-ultramafic rocks, whereas the higher levels of erosion consisted more and more of granitic, pegmatite-rich rocks.

The present geochemical investigation was undertaken to further test the source hypothesis of Viljoen et al. (1970). The study was restricted to pyrite since it forms the most abundant ore mineral in the primary gold ores of the Archean greenstone belts and in the Witwatersrand conglomerates. It was carried out, firstly, by a trace-element investigation of pyrites from the two gold provinces and, secondly, by a comparison of the lead isotopic composition of Witwatersrand pyrites with that of pyrites and lead-bearing sulfides associated with various gold deposits in the Barberton Mountain Land.

PYRITE MINERALOGY

(a) Witwatersrand Basin

In the Witwatersrand ores, pyrite usually exceeds 90 per cent of the ore minerals present and appears to be the only macroscopically identifiable ore mineral (Saager, 1970). It generally occurs disseminated throughout the entire width of individual ore horizons, but in many cases it is concentrated together with other detrital ore minerals (gold, uraninite, chromite, etc.) on false footwalls and on footwall contacts. Between 50 and 75 per cent of the pyrite in the reef horizons possess a rounded shape (Figure 3a).

Witwatersrand pyrites have been classified by Ramdohr (1955) and Saager (1970) (see Table 2). In general, pyrite can be differentiated into the following three groups :

(i) Allogenic pyrites forms the bulk of the rounded grains. They are unweathered, are generally less than 0,2 mm in size, and acquired their roundness by abrasion during sedimentary transport (Figure 3a - 3d). Besides their waterworn shapes, occasional primary inclusions of Ag-rich gold particles possessing a higher reflectivity than the yellow (Ag-depleted) reconstituted gold in the conglomerate matrix, provide further evidence for a detrital origin of these pyrite grains (see also Feather and Koen, 1975). Other primary inclusions in the rounded allogenic pyrite grains, e.g. pyrrhotite, pentlandite, chalcopyrite, and less often, sphalerite, are essentially the same as in the pyrite crystals of the primary gold mineralizations of the Archean greenstone belts.

(ii) Concretionary, authigenic pyrite has diameters several times larger than rounded allogenic pyrite and forms the largest proportion of the "buckshot pyrite" which often are as large as a hazel-

Stratigraphic Position in the Sediments of the Witwatersrand Basin	Detrital Minerals									Main Rock-Types in the Model Provenance-Terrane (Barberton Mountain Land)
	Uraninite	Garnet	Monazite	Cassiterite	Zircon	Gold	Sulfides	Chromite	Platinoids	
Kimberley-Elsburg Group	+				++	++	++	+++	+++	I. Ultramafic Unit (Lower Onverwacht Group) ultramafic-to-mafic lavas; minor felsic tuffs and porphyries; low-volatile tonalitic granite.
Main-Bird Group	+				++	+++	+++	++	+	II. Mafic-to-Felsic Unit (Upper Onverwacht Group) mafic, andesitic, and felsic lavas; felsic-to-mafic pyroclasts; banded chert; low-volatile tonalitic granite; some high-volatile granite (root zone).
Lower Witwatersrand Division	++				++	+	+	+		III. Argillaceous Unit (Fig Tree Group) shales, greywackes, banded ironstone; low-volatile tonalitic granite; high-volatile granite (root zone).
Dominion Reef Group	+++	+++	+++	+++	++	+	+	+		IV. Arenaceous Unit (Moodies Group) quartzites, conglomerates; high-volatile hood granite; pegmatites.

Table 1 : The relative abundance of some heavy minerals in the rudaceous sediments of the Witwatersrand Basin and their correspondent erosion-units in the model source-area of the Barberton Mountain Land (after Viljoen et al., 1970, p. 174). Relative abundance of heavy minerals : + not abundant; ++ fairly abundant; +++ very abundant.

nut. In spite of their generally loose structures and delicate forms, the concretions have distinctly rounded outlines and are very well preserved (Figure 3e, 3f, and 3i). Long transportation distances seem improbable, and Ramdohr (1955) and Saager (1970) have suggested that the concretions were formed *in situ*. Skeletal-type growth structures, e.g. delicate axial crosses, have been found in practically all pyrite concretions and represent characteristic features. Saager and Mihàlik (1967) observed that the concretionary pyrite aggregates very often consist of an isotropic and an anisotropic variety which differ markedly in colour, reflectivity, hardness, and trace content of Ni, Co, and As. The pores in the marginal area of the concretionary pyrite grains sometimes contain numerous fillings of gold, chalcopyrite, and galena. This indicates that the concretions acted as a trap for metamorphically mobilized ore minerals which, subsequent to the deposition of the concretionary grains, infiltrated the pores where they now form inclusions.

In rounded allogenic pyrite grains, inclusions of galena are practically absent.

Rounded pyrite nodules containing microspherical structures of the "mineralized bacteria-type" are closely related to the concretionary pyrite. The microspheres reach diameters of 10-15 microns and, in rare cases, have been observed to be as large as 45 microns. In most cases, the structures are irregularily distributed in the nodules (Figure 3g and 3h). Saager (1970) has suggested that these microspheres may represent organic morphologies. He concluded that the concretionary pyrite

Figure 3(a) :

Typical ore sample from the Basal Reef, showing abraded allogenic pyrite and reconstituted authigenic pyrite which moulds around the rounded grains (white). Note the detrital chromite in the centre of the photograph (dark-grey). Free State Geduld Mine. x200.

Figure 3(b) :

Concentrate of rounded allogenic pyrite from the Leader Quartzite horizon. Welkom Mine. Reflected light, x50.

Figure 3(c) :

Rounded allogenic pyrite with primary inclusions of gangue (black) and gold (bright-white, scratched). Free State Geduld Mine. Reflected light, oil immersion, x500.

Figure 3(d) :

Two rounded allogenic pyrites in gangue from the Basal Reef. Note the fracture-fillings of reconstituted gold and chalcopyrite in the shattered pyrite grain on the left-hand side of the photograph. Free State Geduld Mine. x500.

Figure 3(e) :

Ore sample from the Basal Reef, showing rounded allogenic pyrite (partly cataclastic) and a large porous pyrite concretion. Free State Geduld Mine. Reflected light, x60.

Figure 3(f) :

A large fractured porous pyrite concretion. Free State Geduld Mine. Reflected light, x100.

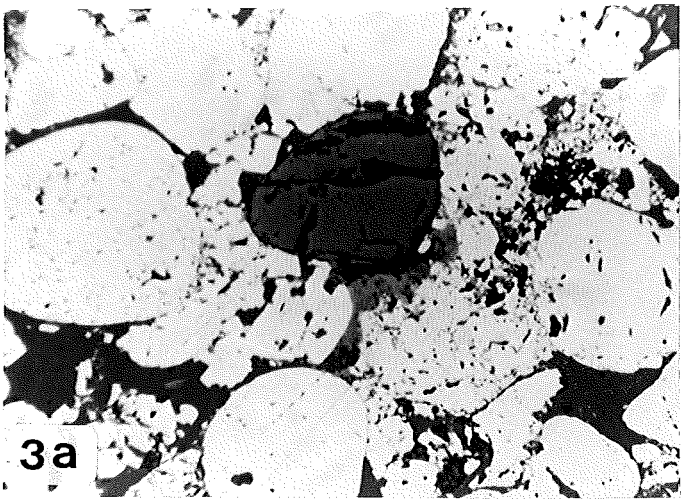
3a

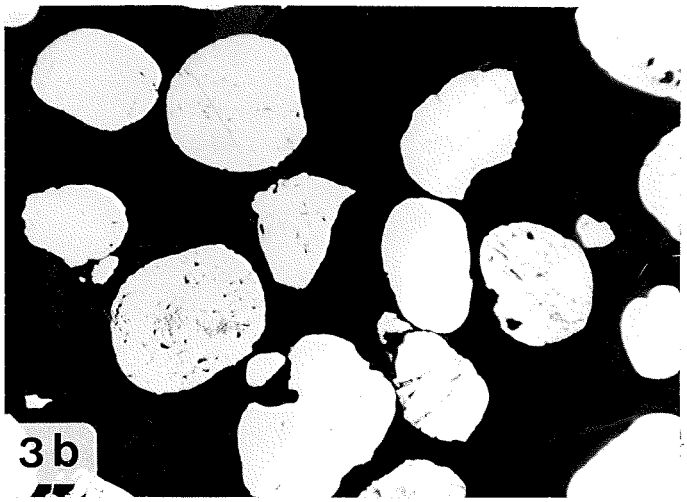
3b

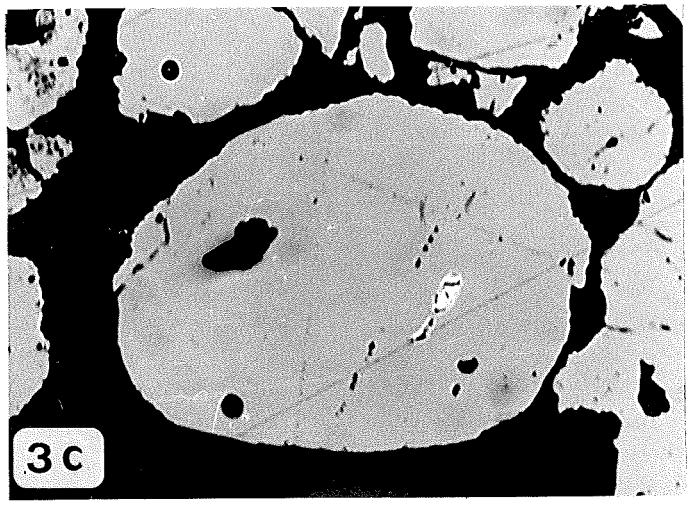
3c

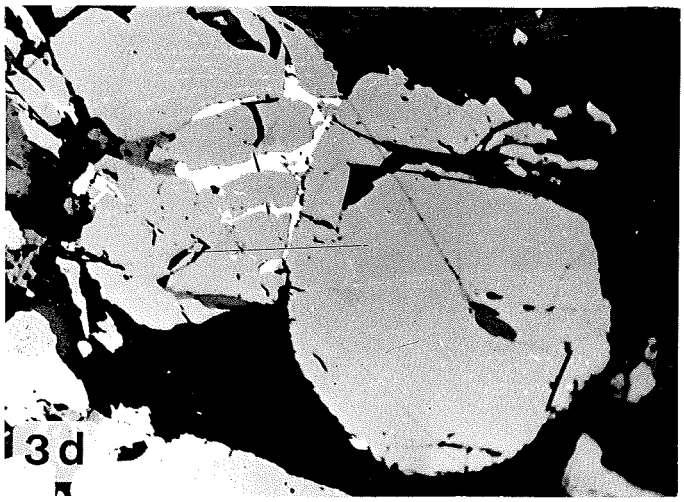
3d

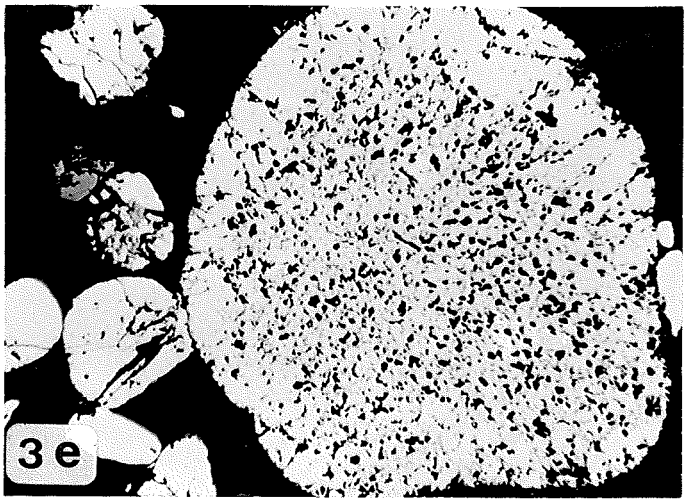
3e

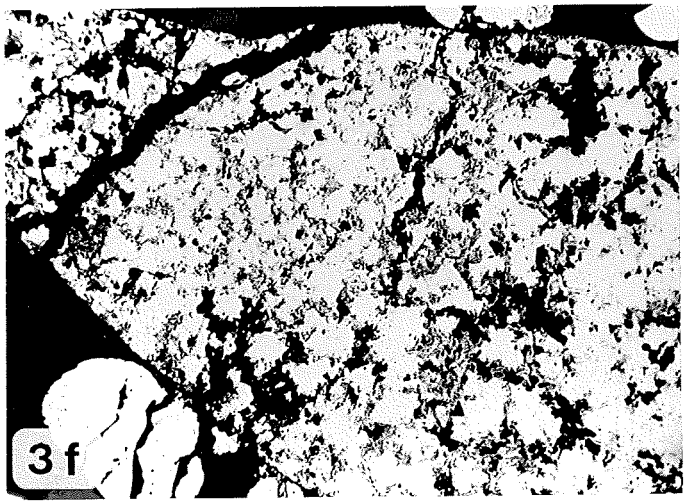
3f

Morphology	Structures	Allogenic	Authigenic
rounded	compact or porous	detrital pyrite and black sands pyritized before their final deposition	black sands pyritized *in situ*
	pseudomorphic	inhomogeneous black sands pyritized before their final deposition	inhomogeneous black sands pyritized *in situ*
	concretionary		generally formed *in situ*; very rarely signs of short transportation
	nodules containing "mineralized bacteria"		formed *in situ*; indication of presence of primitive life
idiomorphic-to-hypidiomorphic	compact or porous		formed *in situ* by reconstitution of ferrous sulfide; rarely hydrothermal along dykes
	compact or porous encrustations		formed *in situ* by reconstitution during metamorphism; generally overgrowth on older detrital pyrites
xenomorphic	veinlets and fracture filling		formed *in situ* by reconstitution during metamorphism

Table 2 : Different pyrite structures in Witwatersrand reefs (after Saager, 1970, p. 32).

and rounded pyrite nodules, as products of precipitation, were formed *in situ* by the activity of anaerobic, H_2S-generating, sulfate-reducing microorganisms which existed in small pocket-like areas in the Witwatersrand Basin.

(iii) Reconstituted authigenic pyrite forms idiomorphic-to-hypidiomorphic grains, or occurs as late encrustations on detrital components of the conglomerate, particularly on pyrite. The pyrite encrustations lead directly to the common stringer-like pyrite veinlets which cut through detrital minerals and form fracture-fillings in other minerals. This authigenic pyrite variety has been formed by recrystallization during the metamorphism of the Witwatersrand sediments (Saager, 1970) (Figure 3k and 3l).

In certain places, dykes intrusive into the Witwatersrand rocks have influenced the content of authigenic minerals and have led to the formation of enriched masses of pyrite, galena, chalcopyrite, and sphalerite. Such occurrences, however, are local and account only for a very small proportion of the authigenic idiomorphic-to-hypidiomorphic pyrite and base-metal sulfides in the Witwatersrand ores (Saager, 1968).

(b) Archean Greenstone Terranes

In the primary gold mineralization of the Archean greenstone belts of the Kaapvaal Craton, pyrite is generally the most abundant ore mineral and often forms the most important carrier of gold. In the gold-vein deposits, generally two generations of pyrite have been observed (Saager, 1973b). The older generation forms large, usually idiomorphic grains measuring up to 10 mm across. They possess abundant inclusions of pyrrhotite, chalcopyrite, and, less commonly, gold, magnetite, rutile, and sphalerite. The younger pyrite generation usually exhibits pentagonal-dodecahedral outlines, with grain-sizes less than 100 microns. It generally surrounds the pyrite of the first generation and rarely contains inclusions of other ore minerals.

A noticeable feature of many pyrites from the greenstone belts is the common occurrence of a distinct zonal structure caused by a variation in the trace-element content of Ni, Co, and As (Figure 3m) (see also Viljoen et al., 1969). Microprobe analyses of the brownish-coloured, softer, weakly anisotropic pyrite zones yield Ni, Co, and As contents of up to 1,75 per cent, 0,17 per cent, and 0,24 per cent, respectively (Figure 4). For a more detailed description of the mineralogy of the gold ores in the Archean greenstone belts, reference can be made to de Villiers (1957), Schweigart and Liebenberg (1966), Viljoen et al. (1969), Saager (1973b), and Liebenberg (1973).

Figure 3(g) :

"Mineralized-bacteria" structures in a large authigenic pyrite concretion from the Basal Reef horizon. Free State Geduld Mine. Reflected light, oil immersion, x500.

Figure 3(h) :

Pyrite aggregate consisting of different-shaped microspherical structures. Note that along the edge of the aggregate some of the globules are distinctly abraded. Free State Geduld Mine. x500.

Figure 3(i) :

Photograph of a polished slab from the Basal Reef. This sample is from the footwall contact and shows an unusually rich concentration of large concretionary pyrite. Free State Geduld Mine. x5.

Figure 3(k) :

Photograph of a polished slab from the Basal Reef horizon. This sample contains predominantly idiomorphic authigenic pyrite in a quartz-pebble conglomerate. Free State Geduld Mine. x5.

Figure 3(l) :

Microphotograph of the authigenic pyrite shown in Figure 3(k). Note the small detrital chromite grains (dark-grey) which are partly overgrown by the reconstituted, in-situ-formed pyrite (white). Free State Geduld Mine. Reflected light, oil immersion, x350.

Figure 3(m) :

Zoned pyrite grains from primary gold mineralization in the Barberton Mountain Land. Sheba Queen Mine. Reflected light, oil immersion, x500.


3 g


3 h

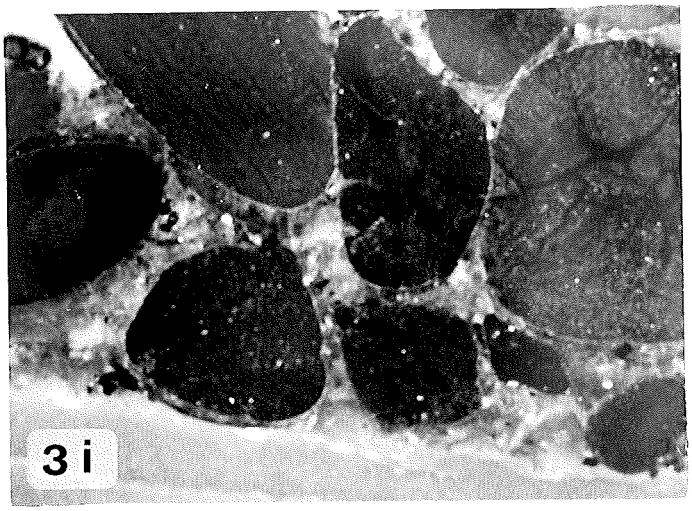
3 i

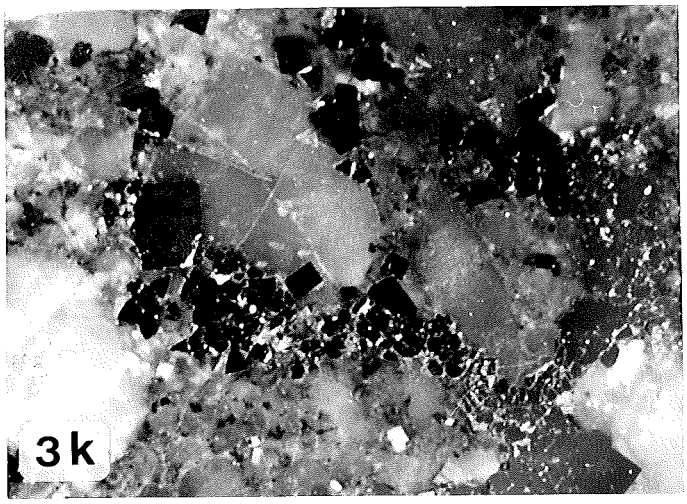
3 k


3 l

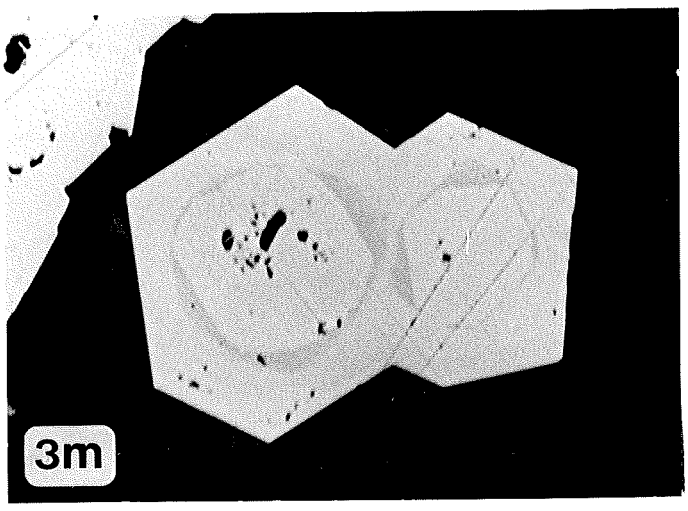
3m

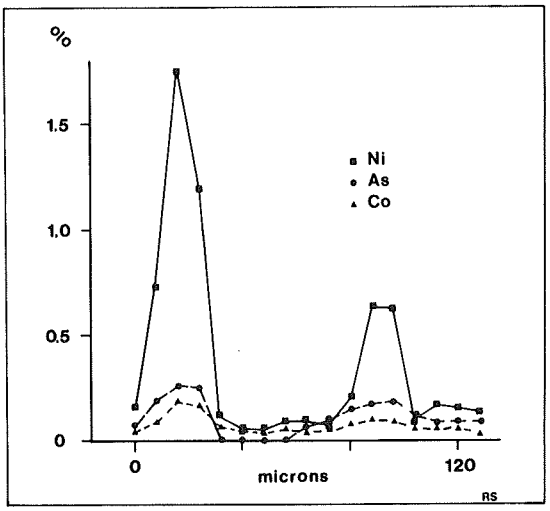

Figure 4 : Electron-microprobe step-scanning profiles through a zoned pyrite from the Eagles Nest Gold Mine in the Barberton Mountain Land. See also Figure 3(m).

SAMPLE PREPARATION

Forty-four pyrite samples from 20 different primary gold mineralizations in the Barberton Mountain Land, the Murchison Range, and the Pietersburg Schist Belt, as well as 13 pyrite samples obtained from reefs of the Central Rand, Klerksdorp, and Orange Free State goldfields, were used for the present investigation. Before concentration, a polished section was made of each ore sample, and the homogeneity and intergrowth relation of the pyrites were studied under an ore microscope.

Most of the ore specimens of primary gold mineralization showed large individual pyrite grains up to 12,5 mm in diameter. They were isolated from the sample by means of a dentist's drill or, after gently crushing and cleaning, the grains were concentrated by hand-picking under a binocular microscope. The concentration of rounded, allogenic Witwatersrand pyrite proved to be more complicated, due to the small grain-sizes of the detrital pyrite (< 0,5 mm) and the presence of the different pyrite varieties. For these reasons, only such samples could be used which had an unusually high content of one only of the various types of pyrite. The scarcity of suitable samples is demonstrated in the fact that, from more than 100 polished-sections investigated, only 5 could be used for the concentration of detrital pyrite. The selected samples were crushed, sieved, and cleaned in a water stream. Following this, concentrates were obtained by heavy-liquid separation and by hand-picking. The much larger grain-sizes of the authigenic Witwatersrand pyrite, notably the concretionary buckshot pyrite, facilitated concentration and allowed a greater number of samples to be investigated.

Following these concentration and separation processes, all the pyrite samples were treated with 20 per cent HCl and again cleaned ultrasonically in distilled water until free of visible turbidity. Polished-sections were then made from about one-half of the concentrates and their purity examined under an ore microscope. From these examinations, it was estimated that the contamination of the pyrite concentrates by silicate minerals or other sulfides was less than 5 per cent by volume and that, for the Witwatersrand samples, the separation of the authigenic from the allogenic pyrite variety was 80-90 per cent successful.

ANALYTICAL PROCEDURE

The Cu-, Zn-, Pb-, Co-, Ni-, and Ag-contents were determined with a Perkin-Elmer Atomic Absorption Spectrophotometer at the University of Heidelberg, and a number of control analyses were carried out by an outside laboratory (Metallgesellschaft, Frankfurt), using photometric and polarographic methods. The limits of detection were 10 ppm for Zn and Ag, 20 ppm for Cu, Co, and Ni, and 50 ppm for Pb. The precisions (two standard deviations) vary between 10 and 30 per cent.

The selection of the elements investigated was based mainly on the following considerations :

(i) Copper, zinc, and lead occur only in restricted amounts as substitutions in the lattice of most natural pyrites (Boyle, 1965; Radcliffe and McWeen, 1969 and 1970; Scott and Barnes, 1972). The observed trace contents of these elements thus indicate the extent to which the investigated pyrites were contaminated by microscopic to submicroscopic inclusions of base-metal sulfides, e.g. chalcopyrite, sphalerite, and galena as the most common ones.

(ii) Nickel and cobalt, in contrast, enter the pyrite structure with ease (Kullerud, 1961; Ramdohr, 1969), and, since Ni-Co-sulfides occur rarely in the investigated ore samples (minute pentlandite exsolutions in pyrrhotite), it can be assumed that the obtained Ni and Co values indicate the overall availability of these two elements during the formation of the pyrite.

(iii) Silver occurs almost exclusively in solid solution with gold. Silver-bearing sulfides have been found only as a few grains in a galena aggregate from the Basal Reef in the Witwatersrand (Saager, 1968). The silver values, therefore, serve as excellent indicators for the amount of gold present as inclusions in the pyrite. Primary gold inclusions in detrital Witwatersrand pyrite contain approximately 10 per cent silver (Saager, 1968). For gold grains in primary ores of the Barberton Mountain Land, Ag-contents of 0,2 to 21,6 per cent have been reported by Liebenberg (1973).

DISCUSSION OF RESULTS

According to the mode of formation and the origin of the sampled pyrites, the geochemical data were divided into the following three groups (see also Table 3) :

Group 1 (G.1) : authigenic Witwatersrand pyrite
Group 2 (G.2) : allogenic Witwatersrand pyrite
Group 3 (G.3) : greenstone belt pyrite

		Co	Ni	Cu	Zn	Pb	Ag
G.1 : 8 samples							
authigenic Witwatersrand pyrite							
	$\bar{x}$ (ppm)	1301	1347	251	56	963	range
	s (ppm)	932	490	109	30	1029	0-390 ppm
	C	0,71	0,36	0,43	0,54	1,07	
G.2 : 5 samples							
allogenic Witwatersrand pyrite							
	$\bar{x}$ (ppm)	216	450	118	64	135	range
	s (ppm)	88	112	63	21	69	0- 10 ppm
	C	0,41	0,25	0,53	0,31	0,51	
G.3 : 44 samples							
greenstone belt pyrite							
	$\bar{x}$ (ppm)	198	514	341	151	123	range
	s (ppm)	195	532	456	379	73	0-380 ppm
	C	0,98	1,04	1,13	2,51	0,59	

Table 3 : Grouped results of trace element analyses. $\bar{x}$ = mean; s = standard deviation; C = coefficient of variation.

Unfortunately, the Ag-values had to be omitted from all further consideration as most of the analyses lie within the limit of detection. For each of the five remaining elements - Co, Ni, Cu, Pb, Zn - and for each of the three groups, the sample cumulative-frequency distribution was constructed (Figure 5). With the aid of the non-parametric Kolmogorov-Smirnov statistic, the various cumulative-frequency distributions were compared with each other, and, for each element, the null hypothesis was

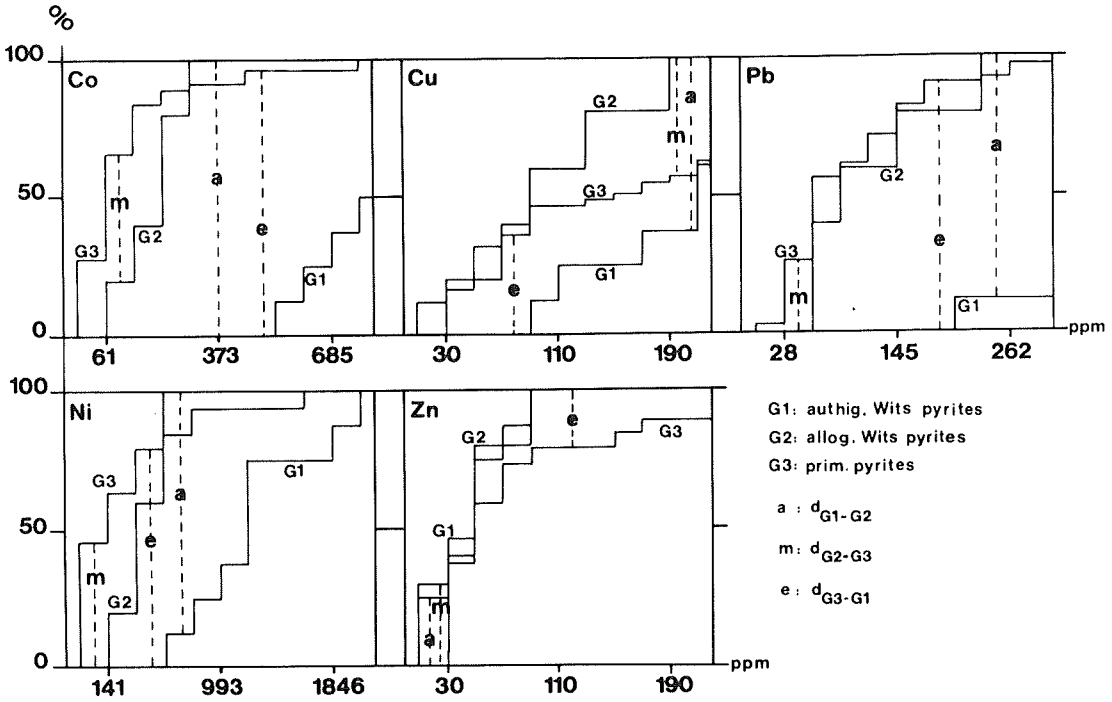

Figure 5 : Cumulative frequency distributions of trace element values from the grouped pyrite samples and graphical solutions of Kolmogorov-Smirnov statistic.

tested that the three sample frequency distributions (e.g. the three postulated pyrite groups) were drawn from populations having the same frequency distribution. The Kolmogorov-Smirnov statistic was employed as no assumptions are needed about the normality of the distributions and as it is not subject to the very small sample limitation of chi-square. The test is a graphic one and the maximum vertical deviation (d_n) between the sample cumulative frequencies is directly measured on the graph (see Figure 5). The obtained d_n values are then compared with values extracted from tables and the null hypothesis either accepted or rejected at a certain level of significance.

The results of the test are shown in Table 4. At a 0,05 level of significance, the measured maximum deviations (d_n) do not in all cases exceed the required values, thus failing to supply evidence that the investigated sample groups were drawn from different populations. It follows that the above proposed grouping of the samples is not always geochemically significant. This is particularly the case for the allogenic Witwatersrand pyrites and the greenstone belt pyrites (G.2-G.3). At a 95 per cent level of probability - with respect to all five investigated elements - the samples were drawn from the same population. It thus can be assumed that both the allogenic Witwatersrand pyrites and the pyrites from greenstone belts have been formed in similar geological environments under similar chemical and physical conditions. These results support the source hypothesis of Viljoen et al. (1969) for an origin of the detrital Witwatersrand pyrite from mineralization in the Archean greenstone terranes of the Kaapvaal Craton.

With respect to the other pairs of pyrite groups (G.1-G.2 and G.1-G.3), viz. authigenic Witwatersrand pyrites and allogenic Witwatersrand pyrites, on the one side, and authigenic Witwatersrand pyrites and greenstone belt pyrites, on the other side, the results are not as distinct and uniform (Figure 5 and Table 4). For the elements Co, Ni, and Pb, the maximum deviations (d_n) exceed the required values, and the postulated sample groupings seem to be justified. The distribution of the elements Cu and Zn, however, deviate very little, and, at a 0,05 level, it can be assumed that the samples were drawn from the same population. The proposed grouping, with respect to Cu and Zn, seems to be invalid.

These contradictory results require further comment :

(i) The Cu- and Zn-trace contents of the pyrites, as explained above, have been caused by inclusions of base-metal sulfides and, thus, are an indication of the contamination of the pyrite by

Pyrite Groups	G.1 - G.2	G.2 - G.3	G.1 - G.3
Minimum Deviation Required at Given Level	$sign._{0,05}$ = 0,700	$sign._{0,05}$ = 0,580	$sign._{0,05}$ = 0,590
Co	$d_{G.1-G.2}$ = 1,000 H_o : G.1 ≠ G.2	$d_{G.2-G.3}$ = 0,475 H_o : G.2 = G.3	$d_{G.1-G.3}$ = 0,955 H_o : G.1 ≠ G.3
Ni	$d_{G.1-G.2}$ = 0,875 H_o : G.1 ≠ G.2	$d_{G.2-G.3}$ = 0,455 H_o : G.2 = G.3	$d_{G.1-G.3}$ = 0,785 H_o : G.1 ≠ G.3
Cu	$d_{G.1-G.2}$ = 0,625 H_o : G.1 = G.2	$d_{G.2-G.3}$ = 0,425 H_o : G.2 = G.3	$d_{G.1-G.3}$ = 0,355 H_o : G.1 = G.3
Zn	$d_{G.1-G.2}$ = 0,250 H_o : G.1 = G.2	$d_{G.2-G.3}$ = 0,290 H_o : G.2 = G.3	$d_{G.1-G.3}$ = 0,210 H_o : G.1 = G.3
Pb	$d_{G.1-G.2}$ = 0,875 H_o : G.1 ≠ G.2	$d_{G.2-G.3}$ = 0,270 H_o : G.2 = G.3	$d_{G.1-G.3}$ = 0,920 H_o : G.1 ≠ G.3

Table 4 : Results of Kolmogorov-Smirnov statistic.

other sulfides. Inclusions of chalcopyrite and sphalerite have been observed irregularly distributed in the pyrites of all three postulated sample groups. They are primary inclusions which formed as mechanical admixtures (Ramdohr, 1969) during pyrite crystallization or are infiltrated secondary inclusions which migrated into the marginal areas of porous pyrites during metamorphic periods. Both types of inclusions are not characteristic of a specific pyrite group, and this is reflected in the Kolmogorov-Smirnov test.

(ii) Co and Ni in pyrite show a different crystal-chemical behaviour, occurring in solid solution. Thus, the trace contents of these two elements are an indication of the availability of Co and Ni during pyrite formation. It follows that the two elements represent better indicators for the study of the metallogenic origin of the investigated pyrites. Carstens (1941), Hegemann (1943), Cambel and Jarkovsky (1967), and other workers have stated that sedimentary and hydrothermal pyrites possess different and characteristic Co- and Ni-trends. Sedimentary pyrites have low Co/Ni ratios, with rather constant Co- and Ni-contents of about 10 ppm and 200 ppm, respectively. In contrast, hydrothermal pyrites have more erratic and considerably larger (several 1 000 ppm) Co- and Ni-contents, with Co/Ni ratios which are greater than 0,1 and as high as 830 (Berg and Friedensburg, 1944). Hawley and Nicol (1961) indicated that pyrites from magmatic ores usually show higher Co- and Ni-contents than pyrites from hydrothermal ores, and Wilson (1953), on the basis of relative availability, concluded that pyrite derived from early magmatic melts would have a higher Ni-content, and probably a lower Co/Ni ratio, than pyrite formed from late fluids. Recent investigations (Tourtelot, 1964; Roscoe, 1965; Saager, 1965; Loftus-Hills, 1967) suggest that the above criteria are only valid in a generalized way and cannot be used to distinguish between different types of ore deposits. The studies, however, indicate that in many cases pyrites from specific occurrences or metallogenic provinces exhibit characteristic and persistent Co- and Ni-trends which agrees with the present study and which also explains why the elements Co and Ni yielded the best results in the Kolmogorov-Smirnov test.

(iii) The very high Pb-contents (between 230 and 3 400 ppm) are significantly restricted to the authigenic Witwatersrand pyrites (see Table 3) because the usually very porous pyrites quite commonly have metamorphically infiltrated galena inclusions in their marginal zones, and it can be assumed that the lead in these inclusions is of radiogenic origin (Saager, 1970; Burger et al., 1962). The allogenic Witwatersrand pyrites which are very compact (Saager, 1970) and practically free of galena inclusions of infiltrated radiogenic lead possess Pb-contents of less than 240 ppm. Similar low Pb-contents were found in the pyrites from the greenstone belts which have been formed in a geological environment characteristically devoid of Pb-bearing minerals (de Villiers, 1957; Saager and Köppel, 1976). It is for these reasons that the Pb-values yielded the same statistical trend as displayed by the Co and Ni data, in spite of the fact that the crystal-chemical behaviour of Pb is markedly different from that of Ni and Co.

FACTOR ANALYSIS

To further investigate the trace element data of the pyrites and to test the results of the graphic Kolmogorov-Smirnov statistic, a factor analysis of the data was carried out. Factor analysis is a branch of multivariate statistics which recently has found increasing application in various fields of the earth sciences. The primary aim of the analysis is to investigate the intercorrelations within a set of data and to find an as-small-as-possible noncorrelated set of basic vectors, which accounts for most of the variance in the original set of data. Factor analysis, therefore, tries to simplify a complex set of data by expressing it in a minimal number of theoretical variables or factors without significant loss of information. The factors which are linear combinations of the original variables must be interpreted in terms of all available geological and other information. The Q-mode factor analysis, as employed in this study, examines the variation from sample to sample, and its objective is to find groups of samples that are similar to one another in terms of their total composition. The observed variations from sample to sample are not independent but are dependent upon underlying causes. If these causes are the same for two samples, then the values measured in these samples will be similar. The similarity measure used in the Q-mode analysis is the cosine "theta" of the angle between two sample vectors in n-dimensional space. All the obtained cosines yield the cosine "theta" or similarity matrix. It is analysed mathematically and the principal components or factors extracted by simultaneous consideration of all the sample similarities. Once the minimum number of factors required has been established, the factors are rotated according to specific mathematical criteria - in the present study, the varimax rotation - to aid interpretation of geological data.

The Q-mode factor analysis was carried out at the Computing Centre of the University of Heidelberg, using a modified FORTRAN program written by J.D.S. Wilson, Department of Geology, University of British Columbia.

The results of the analysis showed that a 2-factor model accounts for 69,8 per cent of the total variance in the original pyrite data. The composition of the two factors or end-members can be roughly determined by scanning down the columns of the factor-score matrix (Table 5).

	Factor 1	Factor 2
Co	-1,0994	-0,3326
Ni	-1,5330	0,1660
Cu	0,2406	-1,7544
Zn	0,0034	-1,3042
Pb	-1,1863	-0,2646

Table 5 : Varimax factor-score matrix

Factor 1 is essentially a Co-Ni-Pb-factor accounting for 37,2 per cent, and Factor 2 is a Cu-Zn-factor accounting for 32,6 per cent of the available information. This grouping into two factors corresponds closely with the trend found by the Kolmogorov-Smirnov statistic, i.e. it shows the independent behaviour of the elements Co, Ni, and Pb from that of the elements Cu and Zn.

The factor loading of each pyrite sample is the projection of each factor axis on each sample vector or, more simply, the composition of each sample with respect to the extracted 2-factor model (Table 6). The factor loadings, as determined from the Q-mode factor matrix have been plotted on a scatter diagram (Figure 6). The axes of the diagram represent the two factors and the units on the axes are given in factor loadings. They vary between - 1,0 and +1,0. The sum of the squared factor loadings of each sample gives the communality. This value indicates, for each sample, what proportion of the variance has been explained by the factor model employed. The communality has a value of 1,0 if the particular sample has been explained at the 100 per cent level by the extracted factors (Table 6). The scatter diagram (Figure 6) demonstrates the heterogeneous distribution of all the investigated trace elements in the greenstone belt pyrites (see also Table 3). These pyrites originated from a large number of genetically different mineralizations which occurred in quite different geological environments. The generally low Co-, Ni-, and Pb-contents of these samples are reflected in the weak, but distinct, accumulation of data points in the positive half of Factor 1.

The allogenic Witwatersrand pyrites show a rather similar, irregular distribution on the diagram. Only one sample, F.III, exhibits a certain affinity with the data points of the authigenic Witwatersrand pyrite, possibly reflecting an imperfect separation of the two pyrite varieties during sample preparation.

Sample No.	Communality	Factor 1	Factor 2
B.24	0,7580	-0,5682	-0,6594
SW.8	0,9632	0,3311	0,9239
SW.1	0,9294	-0,8541	0,4472
EN.4	0,3685	-0,4252	0,4333
EN.85	0,8799	0,4970	0,7955
ST.29d	0,6562	-0,0182	0,8099
SG.29	0,8044	-0,3615	0,8205
SB.191	0,2739	0,4096	0,3257
528	0,8199	0,3324	0,8423
NO.3	0,6467	0,0690	0,8012
25	0,8154	0,4806	0,7645
BR.9	0,5274	0,6046	0,4025
3.3	0,9028	-0,9500	-0,0197
3.4	0,5997	-0,7398	-0,2288
BS.184	0,7320	-0,8163	-0,2562
2.HH	0,9046	-0,9473	-0,0845
SB.231	0,8854	0,9278	-0,1566
H.231	0,7985	0,7922	-0,4133
H.401	0,2412	0,2774	-0,4052
120	0,8199	0,3324	0,8423
F.III	0,4721	-0,6855	-0,0472
	Variance	37,1910%	32,6009%
	Cum. Var.	37,1910%	69,7919%

Table 6 : Partial Q-mode varimax factor matrix

The authigenic Witwatersrand pyrites, in contrast, are far more homogeneous and exhibit a distinct cluster (Figure 6). With respect to the investigated system, these samples possess a very high degree of similarity. As all authigenic Witwatersrand pyrites have comparatively high Co-, Ni-, and Pb-contents, they all plot close to the -1,0 value of Factor 1. The high Co-, Ni-, and Pb-values can be regarded as an indication of the high availability of these elements in the Witwatersrand Basin where the formation of the authigenic pyrite took place, possibly as late as the metamorphism of the sediments (Saager, 1970; Köppel and Saager, 1974). Relatively high Co- and Ni-contents in the Witwatersrand sedimentary material are in good agreement with the source-model of Viljoen et al. (1970) who postulated a granite-greenstone source-terrane which, in its lower members, is largely built up of mafic-to-ultramafic rocks. The high Pb-contents can be explained by the radio-active decay of the U- and Th-bearing placer minerals in the Witwatersrand sediments.

Identical to the results of the Kolmogorov-Smirnov test, the Q-mode factor analysis shows that the allogenic Witwatersrand pyrite and the greenstone-belt pyrites possess geochemical similarities which clearly set them apart from the authigenic Witwatersrand pyrite. The investigation also indicated that pyrites formed in a sedimentary environment possess far more homogeneous trace-element contents than those originating from hydrothermal deposits. This observation agrees with the general trends of the trace-element contents in sedimentary and hydrothermal pyrites.

LEAD ISOTOPE INVESTIGATION

As part of the same research project, various pyrite and galena samples from Witwatersrand reefs and from primary gold deposits in the major greenstone belts of the Kaapvaal Craton were investigated for their lead isotopic composition. The results of the study have been reported in

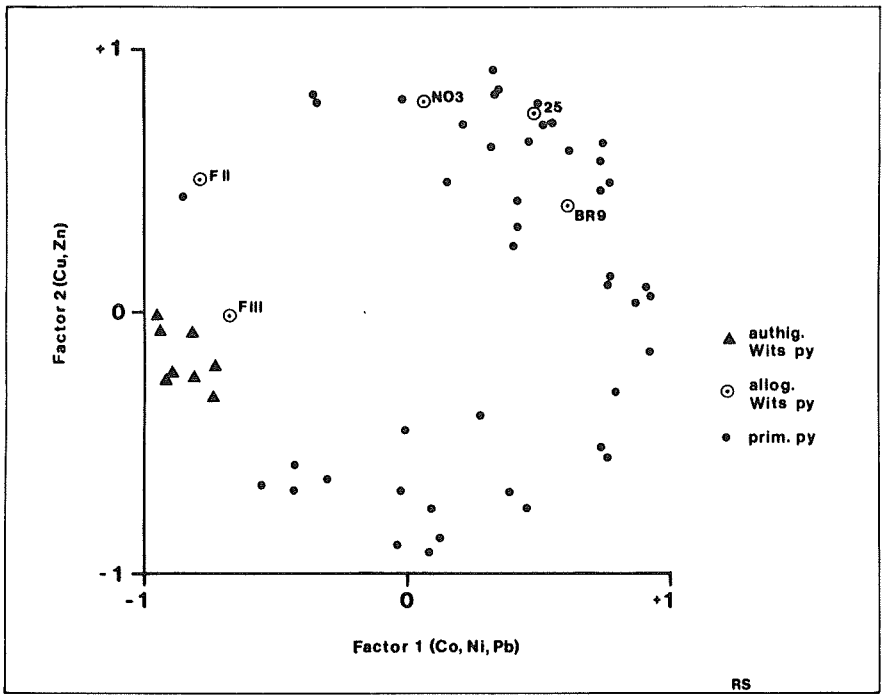

Figure 6 : Scatter diagram of the factor loading values.

detail in an earlier investigation (Köppel and Saager, 1974). They bear additional important information on the provenance of the detrital pyrites in the Witwatersrand sediments and are summarized below.

U-Th-Pb geochronological dating has been undertaken of various sequences of the Witwatersrand Basin. It yielded, for the Dominion Reef Sequence, at the base of the assemblage, a maximum sedimentary age of 2 850 ± 55 m.y. (Allsopp, 1964) and for the Ventersdorp Sequence, which directly overlies the Witwatersrand Sequence, an age of 2 300 ± 100 m.y. (van Niekerk and Burger, 1964). Nicolaysen et al. (1962), by means of U-Pb investigations of rounded uraninite and monazite grains and of total conglomerate samples from the Dominion Reef sediments, showed that these minerals have a crystallization age of 3 080 ± 100 m.y. which is consistent with the hypothesis of a detrital origin of the uraninite and monazite. The U-minerals apparently were reconstituted and suffered a first complete lead-loss 2 040 m.y. ago; a second lead-loss occurred in recent times (Wetherill, 1956; Nicolaysen et al., 1962). Lead isotope studies carried out on galena samples from various reefs of the Witwatersrand deposit by Burger et al., (1962) yielded independent evidence for approximately 3 000 m.y.-old detrital components in the sedimentary filling of the basin. The investigation furthermore confirmed a period of lead-loss 2 040 m.y. ago. This alteration period coincides with the emplacement of the Bushveld Granite at Houtbeck (Nicolaysen et al., 1958) and represents a period of mild regional metamorphism of the Witwatersrand sediments, possibly responsible for the solution stage of the modified placer theory.

The results of the lead isotope study of Köppel and Saager (1974) are condensed on a lead-lead diagram (Figure 7). On this diagram, a hypothetical field is delineated in which all the data points of the authigenic Witwatersrand minerals should plot. The construction of the field necessitated the following assumptions : (i) that the crystallization age of the U-bearing minerals in the sediments is 3 100 m.y., and (ii) that only two periods of lead-loss occurred; the first one 2 040 m.y. ago and the second one in recent times. The upper boundary of the field is then given by the secondary isochron due to the first lead-loss of the 3 100 m.y.-old U-Pb system. This isochron has a slope of 0,384 and corresponds with the "main trend" of Burger et al. (1962). The lower boundary of the field, due to the second lead-loss, starts at the lower end of the upper boundary and has a slope of 0,124 which is the present day Pb 207/Pb 206 ratio of a 2 040 m.y.-old U-Pb system. It is important to note that all the investigated authigenic Witwatersrand minerals of Burger et al. (1962) and of Köppel and Saager (1974) plot within the predicted field. Only two data points from the results of the latter authors are shown, as most samples contain large amounts of radiogenic lead and, thus, plot outside of the diagram (Figure 7) on the open side of the wedge-shaped field.

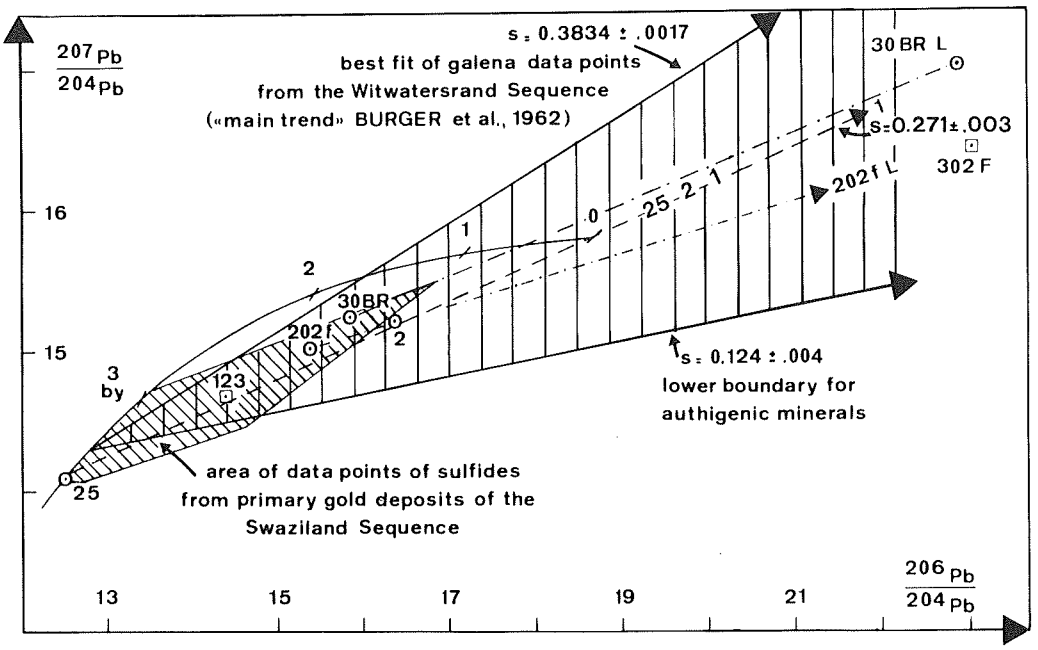

Figure 7 : 207Pb/204Pb versus 206Pb/204Pb diagram. The field of authigenic Witwatersrand minerals is vertically hatched; the field of sulfides from primary mineralization in the Archean greenstone belts is diagonally hatched. Circles denote allogenic pyrite and squared authigenic pyrite from the Witwatersrand sediments. "L" denotes a HCl leach of the sample (after Köppel and Saager, 1974, p. 327).

The following parameters were used for calculating the growth curve :

$(206Pb/204Pb)_o = 9,56$; $(207Pb/204Pb)_o = 10,42$; $T_o = 4,55$; $238U/204Pb = 9,0$

$\lambda_{238} = 1,537 \times 10^{-10} y^{-1}$; $\lambda_{235} = 9,722 \times 10^{-10} y^{-1}$

The field of data points of sulfides from primary gold ores in the greenstone belts was experimentally determined (Saager and Köppel, 1976). It does not completely overlap the field of authigenic Witwatersrand minerals.

The results of Sample No. 25 in this study are of special interest. This is a detrital pyrite sample originating from the Basal Reef horizon of the Free State Geduld Mine in the Orange Free State Goldfield. It has a lead-isotopic composition which, on the diagram (Figure 7) plots outside the predicted field of authigenic minerals. The lead-isotopic composition of this sample concurs with the rounded water-worn shapes of the pyrites, confirming their detrital origin from a source situated outside the Witwatersrand Basin.

The lead-isotopic composition of Sample No. 25, on the contrary, is identical with that observed in galena from the Rosetta Mine, a primary gold lode deposit located in Onverwacht Group rocks of the Barberton Mountain Land. A remarkable lead line was also obtained from the three detrital pyrite samples, No. 25, No. 2, and No. 1 (Sample No. 1 lies outside of the graph), which were collected at the same locality in the Basal Reef. The samples contain all the same first-stage lead, indicating an origin from a lead-source similar to that found in the Archean greenstone terrane. The tie-line of the data points (Figure 7) has a slope of 0,271 which corresponds with the present day Pb 207/Pb 206 ratio of a 3 360 m.y.-old U-Pb system. Slopes yielding such ages were commonly observed by Saager and Köppel (1976) in pyrite samples from greenstone belts and also in whole-rock samples from the Onverwacht Group (Sinha, 1972). Significantly, the age of 3 360 m.y. is identical to the minimum age of the volcanic rocks of the Upper Onverwacht Group of the Barberton Mountain Land, as reported by van Niekerk and Burger (1969).

Sample No. 202(f) and No. 30BR are also detrital pyrite samples from the Klerksdorp and the Orange Free Stage goldfields, respectively. They exhibit lead-isotope compositions similar to those observed in sulfides from primary gold mineralizations in the greenstone belts, but their data

points also fall into the predicted field of authigenic Witwatersrand minerals. However, it is conspicuous that the slopes of the tie-lines to the respective HCl-leaches of the two allogenic pyrite samples are steeper than analogous tie-lines of the authigenic Witwatersrand minerals. The hypothetic first-stage lead of these detrital pyrites resembles that of galenas from primary deposits in the greenstone belts (Figure 7; see also Ulrych et al., 1967).

SUMMARY AND CONCLUSIONS

(i) Compact, rounded pyrite grains from the Witwatersrand sediments and pyrites from primary gold mineralization in greenstone terranes of the Swaziland Sequence exhibit identical heterogeneous trace-element contents. At a high significance level, their Co-, Ni-, and Pb-values were drawn from populations having the same distribution. It follows that both pyrite varieties were formed under similar chemical and physical conditions in a similar geological environment, and that the compact, rounded Witwatersrand pyrites are, in fact, of detrital origin.

(ii) The large, often extremely porous Witwatersrand pyrites, which were formed in the basin of deposition, possess remarkably homogeneous trace-element values and conspicuously high Pb-, Ni-, and Co-contents. These trends clearly differentiate this pyrite variety from the other investigated pyrites and suggest a different mode of formation, probably by a sedimentary process.

(iii) Although comparatively few pyrite samples have been analyzed for their lead-isotopic composition, the results agree with the trends observed in the trace-element investigations. The isotope study provides evidence that the detrital Witwatersrand pyrites derive from a source-area with a lead-isotopic composition identical to that of the greenstone belts of the Swaziland Sequence. The observed leads, furthermore, indicate that the detrital Witwatersrand pyrites were formed at a considerably greater age than the Witwatersrand sediments.

(iv) The provenance-area of the Witwatersrand sediments lay to the northwest of, and close to, the rim of the basin, and was similar to, and of the same age as, the Barberton Mountain Land, a typical Archean granite-greenstone terrane. However, it must be noted that the Barberton Mountain Land, which lies some 300 km east of the Witwatersrand deposits, can be regarded only as a model for the source-terrane, and that the actual provenance-area was closer to the basin. It was either eroded away and/or covered by younger strata.

(v) Pyrite and gold are intimately associated in the primary and the fossil-placer gold province. It can be assumed that, not only the detrital Witwatersrand pyrite, but also the Witwatersrand gold originated from pyritic and often gold-rich mineralizations in the greenstone belts of the Swaziland Sequence. The Au-mineralizations are genetically related to ultramafic and mafic, often Mg-rich, volcanics which are exceptionally abundant in the Lower Onverwacht Group at the base of the Sequence. It is possible that the larger portion of the detrital sulfides came from the acid volcanics of the Upper Onverwacht Group.

(vi) The detrital U- and Th-bearing minerals in the Witwatersrand sediments possess a crystallization age of 3 040-3 160 m.y. This agrees well with the U-Pb and Rb-Sr ages reported for some of the granites in the basement of the Kaapvaal Craton. Due to the high thorium content of many uraninites in the Witwatersrand sediments, it has been suggested that they are derived from a granitic or pegmatitic source. According to the provenance model, such source-rocks would have formed the highest erosional levels in a typical Archean granite-greenstone terrane. The model provides an explanation as to why no primary uranium mineralization has yet been found in the granite-greenstone terranes of the Kaapvaal Craton.

(vii) Two geochemically and petrogenetically different rock-assemblages provided the sources for the gold and uranium in the Witwatersrand sediments. Both rock assemblages occupied different erosional levels and, depending upon the prevailing denudation and drainage conditions, varying amounts of gold and uranium were deposited in the basin. The expected trend from U-rich horizons at the bottom of the sedimentary sequence to Au-rich horizons at its top is still observable. Reworking of the sediments, weathering of material, and various other sedimentary processes have led to considerable deviations from this overall trend.

* *

Acknowledgements

The writer is indebted to Drs. M.J. and R.P. Viljoen, of the Johannesburg Consolidated Investment Company Ltd., who gave advice and assistance during the field work. Professor D.A. Pretorius and Dr. C.R. Anhaeusser of the Economic Geology Research Unit, University of the Witwatersrand,

Johannesburg, provided many helpful suggestions. Special thanks are also due to the Anglo American Corporation of South Africa Limited for helping the author to obtain samples from the Witwatersrand gold reefs. The isotopic investigations were carried out at the Laboratory for Isotope Geology and Mass Spectrometry, Federal Institute of Technology, Zürich, and a portion of the study was supported by the Deutsche Forschungsgemeinschaft (Grant Sa 210/1,2), for which the author is grateful.

References

Allsopp, H.L. (1964). Rb-Sr Ages from the Western Transvaal : Nature, London, Vol. 204, p. 361-363.

Anhaeusser, C.R. (1971). Cyclic Volcanicity and Sedimentation in the Evolutionary Development of Archaean Greenstone Belts of Shield Areas : Geol. Soc. Australia, Spec. Publ. 3, p. 57-70.

Becker, G.F. (1909). Origin of the Gold of the Rand Goldfields - Some Features of the Rand Banket : Econ. Geol., Vol. 4, p. 373-384.

Berg, G., and Friedensburg, F. (1944). Nickel und Kobalt - Die metallischen Rohstoffe, irhe Lagerungsverhältnisse und ihre wirtschaftliche Bedeutung : Ferdinand Enke Verlag, Stuttgart, 280 pp.

Boyle, R.W. (1965). Geology, Geochemistry, and Origin of the Lead-Zinc-Silver Deposits of the Keno Hill-Galena Hill Area, Yukon Territory : Geol. Surv. Canada, Bull. 111, 302 pp.

Burger, A.J., Nicolaysen, L.O., and De Villiers, J.W.L. (1962). Lead Isotopic Compositions of Galenas from the Witwatersrand and Orange Free State, and their Relation to the Witwatersrand and Dominion Reef Uraninites : Geochim. Cosmochim. Acta, Vol. 26, p. 25-59.

Cambel, B., and Jarkovsky, J. (1967). Geochemie der Pyrite einiger Lagerstätten der Tschechoslowakei : Slovenska Akademia Vied, Bratislava, 493 pp.

Carstens, C.W. (1941). Über sedimentäre Schwefelkiesvorkommen : Kgl. Norsk. Vidensk. Selsk. Forh., Vol. 14, p. 120-122.

Davidson, C.F. (1957). On the Occurrence of Uranium in Ancient Conglomerates : Econ. Geol., Vol. 52, p. 668-693.

Davidson, C.F. (1960). The Present State of the Witwatersrand Controversy : Min. Mag., Vol. 102, p. 84-95.

Davidson, C.F. (1961). The Witwatersrand Controversy : Min. Mag., Vol. 105, p. 88-90.

De Villiers, J.E. (1957). The Mineralogy of the Barberton Gold Deposits : Geol. Surv. S. Afr., Bull. 24, 60 pp.

Feather, C.E., and Koen, G.M. (1975). The Mineralogy of the Witwatersrand Reefs : Minerals Sci. Engng., Vol. 7, p. 189-224.

Graton, L.C. (1930). Hydrothermal Origin of the Gold in the Rand Gold Deposits, Part 1 : Econ. Geol. Vol. 25 Suppl., 185 pp.

Hawley, J.E., and Nicol, I. (1961). Trace Elements in Pyrite, Pyrrhotite and Chalcopyrite of Different Ores : Econ. Geol., Vol. 56, p. 467-487.

Hegemann, F. (1943). Die geochemische Bedeutung von Kobalt und Nickel im Pyrit : Z. Angew. Mineral., Vol. 4, p. 122-239.

Köppel, V.H., and Saager, R. (1974). Lead Isotope Evidence on the Detrital Origin of Witwatersrand Pyrites and its Bearing on the Provenance of the Witwatersrand Gold : Econ. Geol., Vol. 69, p. 318-331.

Kullerud, G. (1961). The Fe-Ni-S-System. The Cu-Ni-S-System. The Fe-Mo-S-System : Year Book, Carnegie Institution, p. 144-152.

Liebenberg, W.R. (1955). The Occurrence and Origin of Gold and Radioactive Minerals in the Witwatersrand System, the Dominion Reef, the Ventersdorp Contact Reef and the Black Reef : Trans. Geol. Soc. S. Afr., Vol. 58, p. 101-223.

Liebenberg, W.R. (1973). Mineralogical Features of Gold Ores in South Africa. In: R.J. Adamson (Editor), "Gold Metallurgy in South Africa". : Chamber of Mines of South Africa, Johannesburg, p. 352-446.

Loftus-Hills, G. (1967). Cobalt and Nickel in Tasmanian Pyrites. In: "The Geology of Western Tasmania - a Symposium" : University of Tasmania, Hobart, 16 pp.

Mellor, E.T. (1916). The Conglomerates of the Witwatersrand : Trans. Inst. Min. Met., Vol. 25, p. 226-348.

Nicolaysen, L.O., de Villiers, J.W.L., Burger, A.J., and Strelow, F.W.E. (1958). New Measurements Relating to the Absolute Age of the Transvaal System and the Bushveld Igneous Complex : Trans. Geol. Soc. S. Afr., Vol. 61, p. 137-163.

Nicolaysen, L.O., Liebenberg, W.R., and Burger, A.J. (1962). Evidence for the Extreme Age of Certain Minerals from the Dominion Reef Conglomerates and the Underlying Granite in the Western Transvaal : Geochim. Cosmochim. Acta, Vol. 26, p. 15-24.

Pretorius, D.A. (1966). Conceptual Geological Models in the Exploration for Gold Mineralization in the Witwatersrand Basin. In: "Symposium on Mathematical Statistics and Computer Application in Ore Valuation" : S. Afr. Inst. Min. Met., p. 255-266.

Pretorius, D.A. (1974). The Nature of the Witwatersrand Gold-Uranium Deposits : Econ. Geol. Res. Unit, Univ. Witwatersrand, Inf. Circ. 86, 50 pp.

Radcliffe, D., and McWeen, H.Y. (1969). Copper Zoning in Pyrite from Cerro de Pasco, Peru - a Discussion : Am. Mineral., Vol. 54, p. 1216.

Radcliffe, D., and McWeen, H.Y. (1970). Copper Zoning in Pyrite from Cerro de Pasco - Reply : Am. Mineral., Vol. 55, p. 527.

Ramdohr, P. (1955). Neue Beobachtungen an Erzen des Witwatersrandes in Südafrika und ihre genetische Bedeutung : Abh. Dtsch. Akad. Wiss, Berlin, Kl. Math. Natw., Vol. 5, 43 pp.

Ramdohr, P. (1969). The Ore Minerals and their Intergrowths : Pergamon Press, 1 174 pp.

Roscoe, S.M. (1965). Geochemical and Isotopic Studies, Noranda and Matagami Areas : Can. Inst. Min. Met., Bull. 58, p. 965-971.

Saager, R. (1965). Erzgeologische Untersuchungen an kaledonischen Blei, Zink und Kupfer führenden kieslagerstätten im Nord-Rana-Distrikt, Nord-Norwegen : City-Verlag, Zürich, 145 pp.

Saager, R. (1968). Newly Observed Ore-Minerals from the Basal Reef in the Orange Free State Goldfield in South Africa : Econ. Geol., Vol. 63, p. 116-123.

Saager, R. (1969). The Relationship of Silver and Gold in the Basal Reef of the Witwatersrand System, South Africa : Mineral. Deposita, Vol. 4, p. 93-113.

Saager, R. (1970). Structures in Pyrite from the Basal Reef in the Orange Free State Goldfield : Trans. Geol. Soc. S. Afr., Vol. 73, p. 29-46.

Saager, R. (1973a). Metallogenese präkambrischer Goldvorkommen in den vulkano-sedimentären Gesteinskomplexen (greenstone belts) der Swaziland-Sequenz in Südafrika : Geol. Rundschau, Vol. 62, p. 888-901.

Saager, R. (1973b). Geologische und geochemische Untersuchungen an primären und sekundären Goldvorkommen im frühen Präkambrium Südafrikas - Ein Beitrag zur Deutung der primären Herkunft des Goldes in der Witwatersrand Lagerstätte : Unpublished D.Sc. Thesis, Univ. Heidelberg, 150 pp.

Saager, R., and Mihàlik, P. (1967). Two Varieties of Pyrite from the Basal Reef of the Witwatersrand System : Econ. Geol., Vol. 62, p. 719-731.

Saager, R., and Köppel, V.H. (1976). Lead Isotopes and Trace Elements from Sulfides of Archean Greenstone Belts in South Africa - a Contribution to the Knowledge of the Oldest Known Mineralizations : Econ. Geol., Vol. 71, p. 44-57.

Saager, R., and Sinclair, A.J. (1974). Factor Analysis of Stream Sediment Geochemical Data from the Mount Nansen Area, Yukon Territory, Canada : Mineral. Deposita, Vol. 9, p. 243-252.

Schweigart, H., and Liebenberg, W.R. (1966). Mineralogy and Chemical Behaviour of some Refactory Gold Ores from the Barberton Mountain Land : Nat. Inst. Metall., Johannesburg, Res. Rept. No. 8, 72 pp.

Scott, S.D., and Barnes, H.L. (1972). Sphalerite Geothermometry and Geobarometry : Econ. Geol., Vol. 66, p. 653-669.

Sinha, A.K. (1972). U-Th-Pb-Systematics and the Age of the Onverwacht Series, South Africa : Earth Planet. Sci. Letters, Vol. 16, p. 219-227.

Tourtelot, H.A. (1964). Minor-Element Composition and Organic Carbon Content of Marine and Non-Marine Shales of Late Cretaceous Age in the Western Interior of the United States : Geochim. Cosmochim. Acta, Vol. 28, p. 1579-1604.

Ulrych, T.J., Burger, A.J., and Nicolaysen, L.O. (1967). Least Radiogenic Terrestrial Leads : Earth Planet. Sci. Letters, Vol. 2, p. 179-184.

Van Niekerk, C.B., and Burger, A.J. (1964). The Age of the Ventersdorp System : Annals Geol. Surv. S. Afr., Vol. 3, p. 75-86.

Van Niekerk, C.B., and Burger, A.J. (1969). A Note on the Minimum Age of the Acid Lava of the Onverwacht Series of the Swaziland System : Trans. Geol. Soc. S. Afr., Vol. 72, p. 9-21.

Viljoen, R.P., and Viljoen, M.J. (1969). An Introduction to the Geology of the Barberton Granite-Greenstone Terrain : Geol. Soc. S. Afr., Spec. Publ. 2, p. 9-27.

Viljoen, R.P., Saager, R., and Viljoen, M.J. (1969). Metallogenesis and Ore Control in the Steynsdorp Goldfield, Barberton Mountain Land, South Africa : Econ. Geol., Vol. 64, p. 778-797.

Viljoen, R.P., Saager, R., and Viljoen, M.J. (1970). Some Thoughts on the Origin and Processes Responsible for the Concentration of Gold in the Early Precambrian of Southern Africa : Mineral. Deposita, Vol. 5, p. 164-180.

Wetherill, G.W. (1956). An Introduction to the Rhodesia and Witwatersrand Age Patterns : Geochim. Cosmochim. Acta, Vol. 9, p. 220-292.

Wilson, H.D.B. (1953). Geology and Geochemistry of Base Metal Deposits : Econ. Geol., Vol. 48, p. 370-407.

Young, R.B. (1917). The Banket of the South African Goldfields : Gurney and Jackson, Ltd., London.

oOo